Fermilab FERMILAB-CONF-06-224-E

JET PROPERTIES AT THE TEVATRON

Monica D'Onofrio
Institut de Física d'Altas Energies
Universitat Autònoma de Barcelona, Spain
(On behalf of the CDF and D0 Collaborations)

Abstract

The RunII physics program at the Tevatron started in spring 2001 with protons and antiprotons colliding at an energy of $\sqrt{s}$=1.96 TeV. More than 1 fb^{-1} of data have been collected by both the CDF and DØ experiments. In this contribution, some of the new QCD results are presented.

1 Introduction

The Tevatron $p\bar{p}$ Collider is the highest-energy accelerator currently operational. At the end of 2005, the amount of collected data reached 1 fb^{-1}, leading to a new level of QCD precision in hadron collisions. Compared to Run I, the increase in center-of-mass energy, from 1.8 to 1.96 TeV, and the improved acceptance of the detectors, CDF [1] and DØ [2], allow to perform stringent tests of the QCD predictions in extended regions of jet transverse momentum and jet rapidity. In this contribution, a review of some of the most relevant results from both Tevatron experiments is presented.

2 Inclusive jet cross section measurements

The measurement of the inclusive jet production cross section provides a stringent test of perturbative QCD (pQCD) predictions over about nine orders of magnitude. Thanks to the increase of center-of-mass energy in Run II, the jet production rate at high P_T has significantly increased. The high P_T jets tail probes distances down to about 10^{-19} m and it is sensitive to new physics. Run I measurements [3] raised a great interest on an apparent excess at high transverse energy, finally explained within the Standard Model in terms of the limited knowledge of the gluon distribution within the proton at high x [4]. Recent PDF sets, such as CTEQ6 [5] and MRST2004 [6], include Run I jet data in their global fits. In Run II, jets are reconstructed with the Midpoint algorithm [8] and the longitudinally-invariant k_T algorithm [7].

The MidPoint algorithm is an iterative seed-based cone algorithm, that uses midpoints between pairs of protojets as additional seeds in order to make the clusterization procedure infrared safe. A cone size of $R_{cone} = 0.7$ in the $Y - \phi$ plane is used. Two protojets are merged if the common transverse momentum is larger than 75% of that of the jet with less transverse momentum, otherwise two jets are formed and the common towers are assigned to the closest jet. Figure 1 (left) shows the measured inclusive jet cross section production in $p\bar{p}$ collisions at $\sqrt{s} = 1.96$ TeV, for central jets ($0.1 < |Y^{jet}| < 0.7$), based on about 1 fb^{-1} of CDF Run II data and using MidPoint algorithm. As a function of the jet transverse momentum, the measured cross section extends over more than eight orders of magnitude and it is compared to theoretical prediction. The next-to-leading order (NLO) pQCD cross section is obtained with EKS [9] and CTEQ6.1M PDFs, setting the renormalization and factorization scales to $P_T^{jet}/2$. To emulate the effects related to the merging/splitting procedure, the corresponding NLO pQCD calculation merges two partons if they are within $R_{cone} \times R_{sep}$ of each other and within R_{cone} of the resulting jet centroid, where the parameter R_{sep} is set to 1.3. Figure 1 (right) shows the ratio between data

and theory. Good agreement with NLO pQCD prediction is found in the whole jet transverse momentum range. In both figures, the shaded band is the total systematic uncertainty on data. Proper comparisons with the theory require corrections for non-perturbative effects. Those contributions come from the underlying event (UE) and the hadronization processes and they are expecially important for low P_T^{jet}. The corresponding parton-to-hadron correction is defined as the ratio of the predicted inclusive jet cross sections at the hadron level and the one after turning off the interactions between proton and antiproton remnants. PYTHIA 6.203 [10] is employed with a special set of parameters, tuned on Run I CDF data, to reproduce the underlying event activity and denoted as PYTHIA-Tune A [11]. Tune A has been shown to properly describe the jet shapes measured in Run II [12]. The parton-to-hadron level correction has been also evaluated with HERWIG 6.4 [13]. The difference between the two Monte Carlos is considered as systematic uncertainty on the correction, and it is important at low P_T^{jet} (see figure 1-right). The experimental uncertainties are dominated by the uncertainty on the absolute jet energy scale, which is known at the level of ± 2 % at low P_T^{jet} and ± 3 % at high P_T^{jet} [15]. This introduces an uncertainty on the measured cross section that varies between about 20% at low P_T^{jet} and 40% at high P_T^{jet}. An additional ± 6 % normalization uncertainty associated with the luminosity measurement is not included. The main uncertainty in the pQCD prediction comes from the PDFs, especially from the limited knowledge of the gluon PDF at high x.

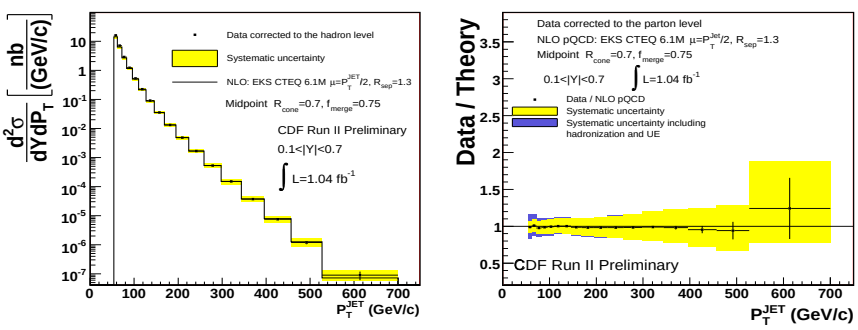

Figure 1: *Inclusive jet cross section measured by CDF for jets with* $0.1 < |Y^{jet}| < 0.7$*, using the MidPoint algorithm. Data are compared to pQCD NLO predictions corrected to the particle level.*

The CDF collaboration has performed a measurement of the inclusive jet cross section implementing the k_T algorithm for jet reconstruction. The k_T

algorithm pairs nearby protojets in order of increasing relative transverse momentum. Inspired by pQCD gluon emissions, it is infrared and collinear safe to all orders in pQCD. Unlike cone based algorithm, it does not include any merging/splitting prescription and it allows a well defined comparison with the theory without introducing any arbitrary parameter. Figure 2 (left) shows the inclusive jet cross section measured for jets searched for using the k_T algorithm with a D parameter of 0.7, where the D parameter approximatly accounts for the dimension of the jet. Five different regions of rapidity are explored, up to $Y_{jet} = 2.1$: precise jet measurements at large rapidities can help constraining the gluon density inside the proton in kinematic regions where no new physics is expected. As in the MidPoint inclusive jet cross section, systematic uncertainties on the data, dominated by jet energy scale uncertainty, are reported as shaded band; the dashed band results from the systematic uncertainty on the theory. The theoretical NLO expectation is superimposed to the measured distributions. The NLO pQCD cross section is obtained with JETRAD [14] using CTEQ6.1M PDFs and setting the renormalization and factorization scales to $max(P_T^{jet})/2$. Parton-to-hadron correction is applied to take into account UE and hadronization effects. The data/theory ratio, presented in figure 2 (right) for the five rapidity regions, shows that the measured cross sections are in good agreement with the QCD prediction. It is particularly important to note that, for the most forward rapidity region ($1.6 < |Y^{jet}| < 2.1$), the uncertainty on the pQCD calculation due to the PDF is larger than the total uncertainty on the data, which indicates that the CDF data will help in further constrain the gluon distribution at high x.

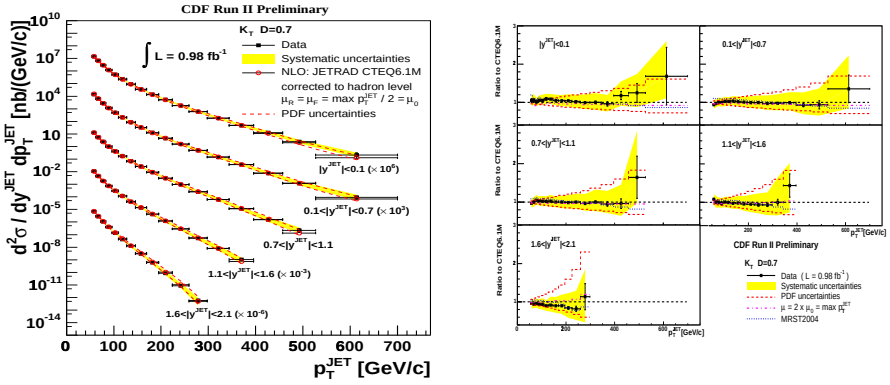

Figure 2: *Inclusive jet cross section measured by CDF for jets in 5 different rapidity regions, up to* $Y_{jet} = 2.1$*, using the longitudinally invariant* k_T *algorithm. It is compared to pQCD NLO predictions corrected to the particle level. (Data/Theory ratio is shown on the right).*

3 Inclusive photon cross section

The cross section [16] for inclusive prompt photon production is measured as a function of the photon transverse momentum, P_T^γ, considering photons with rapidity $|\eta| < 0.9$ and transverse momentum between 23 and 300 GeV/c. The data sample corresponds to an integrated luminosity $L = 326 \pm 21\ pb^{-1}$ accumulated in 2002-2004 with the DØ detector. Prompt photons in hadron collisions are typically produced via quark-gluon Compton scattering or quark-antiquark annihilation. Studies of direct photons with large transverse momenta provide precision tests of pQCD as well as information on the distribution of partons within the protons, particularly the gluon. Photons from energetic π_0 and η mesons are the main background at low P_T^γ; isolated electrons from the electroweak production of W and Z bosons contributes to the background at high P_T^γ. A neural network is used to estimate the purity (P) of the photon sample, defined as the ratio of the signal to signal plus background and statistically determined for each P_T^γ bin. The purity uncertainty is dominated by Monte Carlo statistics at low P_T^γ and data statistics at high P_T^γ.

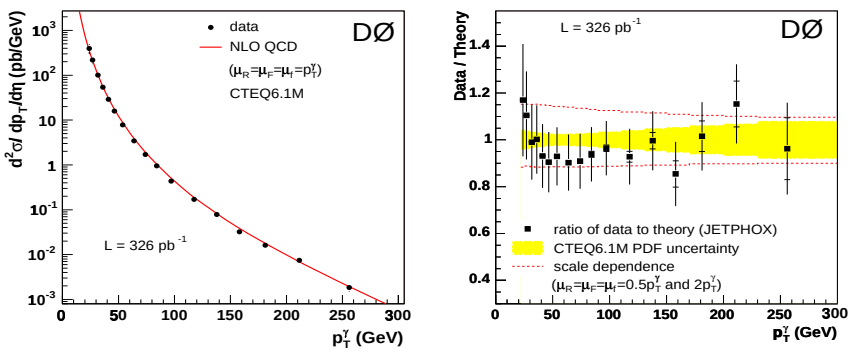

Figure 3: *On the left: inclusive isolated photon cross section compared to pQCD NLO predictions performed with* JETPHOX. *On the right: Ratio Data/Theory.*

The measured cross section is compared to a NLO pQCD calculation (JETPHOX [17]) in Figure 3 (left). Source of systematic uncertainty on the measured cross section include luminosity, energy calibration, photon conversion, trigger efficieny and photon selection efficiency. The theoretical calculation is derived using the CTEQ6.1M PDF for the proton and the BGF [18] fragmentation functions for the photons. The renormalization, factorization and fragmentation scales have been chosen to be equal to the photon transverse momentum ($\mu_R = \mu_F = \mu_f = P_T^\gamma$). As shown in Figure 3 (right), the theoret-

ical calculation agrees with the measured cross section. The scale dependence in the NLO pQCD theory, estimated by varying scales by factors of two, are displayed as dashed lines, the filled area represents the uncertainty associated with the PDFs. Thanks to the lower systematic uncertainties on the photon energy scale, measurement of inclusive prompt photon cross section with a larger amount of data will help to further constrain the gluon distribution within the proton.

4 Inclusive b-jet production cross section

Measurements on bottom-quark production at $p\bar{p}$ collisions provide an important test of perturbative QCD. The observed discrepancy between the measured inclusive B meson cross section and the pQCD predictions in Run I [19] motivated further theoretical developments beyond next-to-leading order [20], that result in a good description of recent B hadron production measurements in Run II [21]. The measurement on b-jet production is performed for jets with rapidity, Y^{jet}, in the range $|Y^{jet}| < 0.7$ and transverse momentum, P_T^{jet}, in the region $38 < P_T^{jet} < 400$ GeV/c, for events in which the decay vertex of the B hadron is directly reconstructed. The cone-based iterative MidPoint algorithm is used for jet reconstruction in the Y-ϕ space, using a cone radius of 0.7. The jet energy scale is corrected, using a Monte Carlo simulation, to compensate for energy losses at calorimeter level. The analysis exploits the good tracking capabilities of the detector and rely on b-jet identification done by secondary vertex reconstruction. The b-tagging algorithm uses displaced tracks associated with a jet that are within the jet cone. The search for secondary vertices is defined in two steps: a first attempt to reconstruct a secondary vertex is performed using at least three tracks with $p_T > 0.5$ GeV/c and impact parameter significance, d_0/σ_{d_0}, above 2.5. If no secondary vertex is found, a second iteration is carried out using only two tracks with $d_0/\sigma_{d_0} > 3$ and $p_T > 1$ GeV/c, where one of the tracks must have $p_T > 1.5$ GeV/c. Once a secondary vertex is reconstructed, an additional requirement is imposed on the two-dimensional decay length, L_{2D}, calculated as the projection onto the jet axis, in the r-ϕ plane, of the vector pointing from the primary vertex to the secondary vertex. The jet is required to have $L_{2D}/\sigma_{L_{2D}} > 7$, where the cut is optimized according to Monte Carlo studies, and $\sigma_{L_{2D}}$ is the total uncertainty on L_{2D}. The heavy-flavor tagged sample, as defined with this algorithm, includes background contributions from charm, gluon and light-quark jets, that can be separated from the b-jet signal using the distribution of the measured secondary vertex mass. Although a full reconstruction of the hadron invariant mass is not possible, due to the presence of neutral particles and energy lost because of detector resolution, the invariant mass of tracks used to find

the secondary vertex constitutes a good discriminator for jets from long-lived B or charm hadrons. The mass of secondary vertex, M_{secvtx}, is fitted to a linear combination of b- and non b-jet Monte Carlo templates, as determined from PYTHIA, and depends on jet transverse momentum. The measured b-jet production cross section is corrected for smearing effects back to the hadron level: it is shown in Figure 4 (left), compared to pQCD NLO predictions [22]. The measured cross section decreases by more than six order of magnitude as P_T^{jet} increases from 38 to 400 GeV/c. The shaded band is the total systematic uncertainty on the data, dominated by uncertainties on the jet energy scale, in addition to uncertainties on the b-tagging efficiency and the fraction of b-jets. The theoretical prediction is computed using a b-quark bare mass m_b=4.75 GeV/c^2, CTEQ6M PDFs and the renormalization and factorization scales, μ_R and μ_F, set to $\mu_0 = 1/2\sqrt{(p_T^{b-jet})^2 + m_b^2}$. At the parton level, the theoretical cross section is determined using a cone-based algorithm with effective cone size $R' = 0.7 \times R_{sep}$, with $R_{sep} = 1.3$. As in the case of inclusive measurement, the pQCD NLO prediction includes an additional correction factor to account for non-perturbative contributions from the underlying event and hadronization processes.

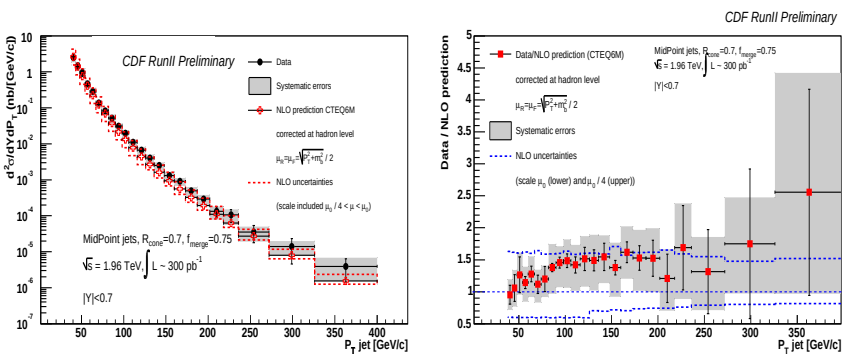

Figure 4: *On the left: Measured inclusive b-jet cross section (filled circles) as a function of* P_T^{jet} *compared with NLO pQCD prediction (empty crosses). On the right: Ratio Data/Theory as a function of* P_T^{jet}*. In both figures, shaded band is the total systematic uncertainty on data, dashed band results from the systematic uncertainty on the theory.*

Figure 4 (right) shows the ratio of data/theory as a function of P_T^{jet}. The uncertainty on the theory (dashed band on both figures) is dominated by its dependence on the renormalization and factorization scales, in addition to the PDF set used in the calculation. The strong dependence observed on the

scales suggests that next-to-NLO contributions might be significant [22]. The measured b-jet cross section is consistent with the theoretical predictions in the whole P_T^{jet}.

5 Jet production in association to W/Z bosons

The study of W and Z bosons production in association with high energy hadronic jets is fundamental since it constitutes a major background for top quark physics as well as Higgs and SUSY searches. The presence of a massive bosons ensures that the hard scattering process has occured at a scale that allows perturbative QCD prediction, thus these measurements offer an ideal ground for QCD studies for what concerns the proper matching procedures between matrix element calculations and parton shower programs to avoid double counting of gluon radiations.

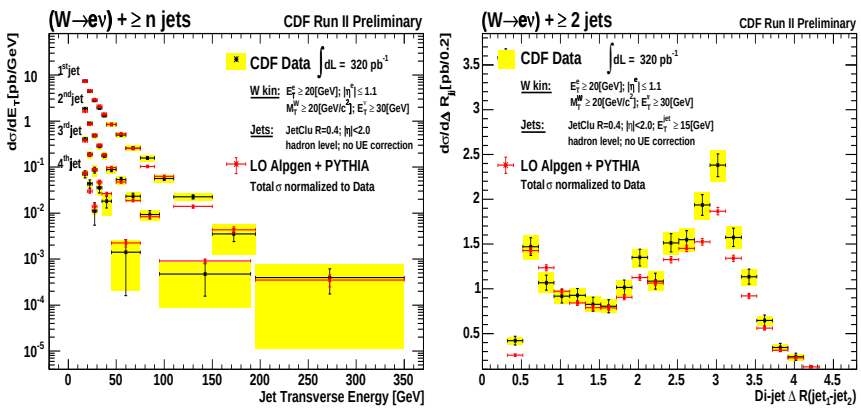

Figure 5: *The measured inclusive differential $W+\geq n$ jets cross section, as a function of jet transverse energy (on the left), and differential ΔR_{jj} cross section in $W+\geq 2$ jets. The measured distribution are compared, in shape, to LO* ALPGEN+PYTHIA *predictions.*

Figure 5 (left) shows the measured inclusive differential cross sections for $W+\geq n$ jets in $p\bar{p}$ collisions at $\sqrt{s} = 1.96$ TeV, as a function of the transverse energy of the jets, based on 320 pb^{-1} of CDF Run II data. W boson candidates are identified via the presence of a high P_T electron and large missing transverse energy associated to the neutrino. The definition of the measured cross section is restricted to the region of phase-space where electron P_T^e is above 20 GeV/c, P_T^ν of the neutrino is 30 GeV/c and the transverse mass of the reconstructed W is above 20 GeV/c^2. Jets are searched for using a cone-based algorithm

with cone size R = 0.4. Only jets with $E_T^{jet} > 20$ GeV and $|\eta^{jet}| < 2.0$ are considered. Figure 5 (right) shows, for $W+\geq 2$ jets, the measured differential cross section as a function of ΔR_{jj}, where ΔR_{jj} denotes the separation (in the η-ϕ space) between the two leading jets. The shaded bands is the total systematic uncertainty, dominated by the jet energy scale uncertainties. The shapes of the measured cross section are compared to pQCD LO predictions as determined using the Matrix Element plus Parton Showering (ME+PS) Monte Carlo ALPGEN(v2) [23]+PYTHIA. CTEQ5L PDF and $\mu^{R/F} = \sqrt{M_W^2 + \sum P_{T,jet}^2}$ are used for renormalization and factorization scales. The predictions, normalized to the total data cross sections, well reproduce measured cross sections.

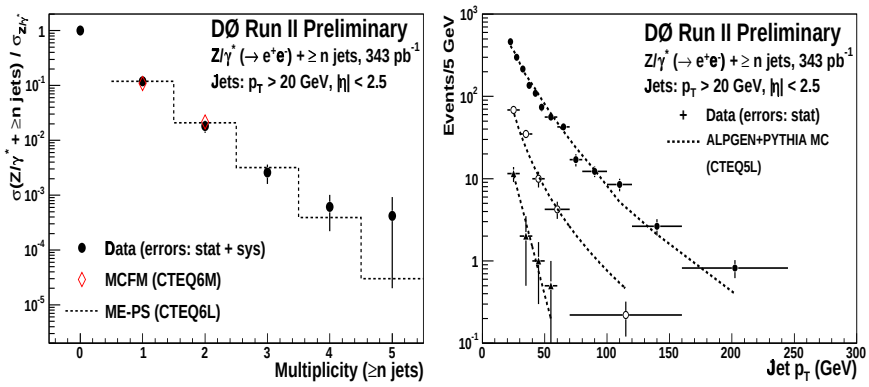

Figure 6: *On the left: Ratio between $Z/\gamma+\geq n$ jet production cross sections and the inclusive Z/γ cross section, as a function of n-jets, compared to two QCD predictions,* MCFM *and 7* MADGRAPH+PYTHIA. *On the right: shape comparison of jet* P_T *spectra of the nth jet with ME+PS* ALPGEN+PYTHIA.

The DØ Collaboration has performed a study of events with Z bosons and hadronic jets using 343 pb^{-1} of integrated luminosity. Ratios of the $Z/\gamma(\rightarrow e^+e^-)+\geq n$ jet cross sections to the total inclusive $Z/\gamma(\rightarrow e^+e^-)$ cross section have been measured for $Z/\gamma+\geq 1$ to 5 jet events. Electron pairs are required to be in the central region of the calorimeter ($|\eta| < 1.1$), and to have an invariant mass near the world average Z boson mass, $75\,\mathrm{GeV/c^2} < M_{ee} < 105\,\mathrm{GeV/c^2}$. Jets are reconstructed using a cone algorithm which combines particles within a cone of radius $R_{cone} = 0.5$, and are required to have transverse momentum above 20 GeV/c and $|\eta| < 2.5$. The cross sections as a function of jet multiplicity are corrected for jet reconstruction and electron identification efficiencies, and for event migration due to the finite jet energy resolution of the detector. Figure 6 (left) shows the fully corrected $Z/\gamma+\geq n$ jet production cross

sections as a function of n, normalized with respect to the inclusive Z/γ cross section for the mass region $75\,\mathrm{GeV/c^2} < \mathrm{M_{ee}} < 105\,\mathrm{GeV/c^2}$, and compared to two QCD predictions, MCFM and a LO calculation (ME+PS). MCFM [24] is a NLO calculation up to Z+2 partons processes. CTEQ6M PDF are used, and factorization and normalization scales are set to $\mu^{\mathrm{R/F}} = \sqrt{\mathrm{M_Z^2} + \mathrm{P_{T,Z}^2}}$. The ME+PS prediction is based on MADGRAPH [25] Z+n partons LO Matrix Element predictions using PYTHIA for parton showering and hadronization. CTEQ6L PDF are also used in this case, factorization scale is set to $\mu_{\mathrm{F}} = \mathrm{M_Z}$, normalization scale to $\mu_{\mathrm{R}} = \mathrm{P_T^{jet}}$ for jets from initial state radiation and $\mu_{\mathrm{R}} = k_{\mathrm{T}}^{\mathrm{jet}}$ for jets from final state radiation. Both predictions, normalized to the measured $Z/\gamma+\geq 1$ jet cross section ratio, agree well with measured data. Figure 6 (right) compares the shape of jet $\mathrm{P_T}$ spectra of the nth jet in $Z/\gamma+\geq n$ jet events to MC predictions based on ALPGEN+PYTHIA, with CTEQ5L PDF and $\mu^{\mathrm{R/F}} = \sqrt{\mathrm{M_Z^2} + \sum \mathrm{P_{T,jet}^2}}$: good agreement is observed.

6 Inclusive b-jet production in association to Z bosons

Both CDF and DØ collaborations have performed measurement on inclusive b-jet production in events with a Z boson in the final state. The inclusive Z + b-jet process is an important background to searches for the Higgs boson in associated ZH production. The process $bg \to Zb$, where the initial b is from the sea of the proton parton distribution, is predicted to account for approximatly two thirds of the total inclusive cross section $\sigma(p\bar{p} \to Z + b\,jet)$ at $\sqrt{s} = 1.96$ TeV, thus it is sensitive to the b-quark density of protons. For this measurement, CDF uses about 325 $\mathrm{pb^{-1}}$ of data collected, DØ about 180 $\mathrm{pb^{-1}}$. Both experiments consider $Z \to e^+e^-$ and $Z \to \mu^+\mu^-$ decay modes for the Z boson. Jets are searched for using the JetClu algorithm ($\mathrm{R_{cone}}$=0.7) for CDF, the MidPoint algorithm ($\mathrm{R_{cone}}$=0.5) for DØ, and are required to be in the tracking coverage region ($|\eta| < 1.5$), with transverse energy(momentum) above 20 GeV. B-jet candidates are identified as jets containing reconstructed secondary vertices. These are more often formed in b-jets than in charm and light quark jets due to the long lifetimes of B hadrons. CDF distinguish the residual light and charm jets on the basis of the mass of all charged tracks used to reconstruct the secondary vertex (see also section 4) and no assumption is made on the relative charm content. DØ assumes from NLO pQCD the ratio of b and charm jets ($\mathrm{N_c} = 1.96\mathrm{N_b}$ [26]). CDF reports the inclusive cross section $\sigma(Z + b\,jet) = 0.96 \pm 0.32(\mathrm{stat.}) \pm 0.14(\mathrm{syst.})$ pb, in reasonable agreement with theoretical expectation of 0.52 pb [26]. Main sources of systematic uncertainties are related to the jet energy scale, to the b-tagging efficiency and to the uncertainty on the amount of jets with two heavy quarks inside

the cone. Both experiments provide a measurement of the ratio of production cross sections of inclusive Z + b-jets to Z+jets, that benefits from cancellations of many systematic uncertainties, such as luminosity uncertainty. The ratio is found to be 0.0237±0.0078(stat.)±0.0033(syst.) for CDF measurement, $0.021 \pm 0.004(\text{stat.}) \pm^{0.002}_{0.003}(\text{syst.})$ for the DØ one, in good agreement with NLO prediction of 0.018±0.004 [26], performed using CTEQ6 parton distributions and renormalization and factorization scales $\mu_R = \mu_F = M_Z$.

7 Conclusions

A very intense physics program is carried out at the Tevatron by CDF and DØ experiments: the amount of collected data, that exceeds 1 fb^{-1}, is leading to a new level of QCD precision studies. Measurements of the inclusive jet cross section have been carried out implementing different jet algorithms and show a good agreement with NLO perturbative QCD prediction. For jets in the forward rapidity region, the measured cross section will help to constrain the gluon PDF at high x. Further informations on the distribution of partons within the protons will be given by the measurement of inclusive prompt photon production with larger amount of data. Measurement of the inclusive b-jet production also provides an important test of perturbative QCD: the cross section is found in agreement with the NLO calculation, although the strong dependence observed on the renormalization and factorization scales suggests that Next-to-NLO contributions might be significant. Better knowledge of the b-quark density of the proton could arise from cross section measurements of b-jets produced in association to a Z boson, found in agreement with NLO prediction although very limited in statistics. Finally, the measurement of W and Z bosons production cross sections in association with high energy hadronic jets has been performed. Results, compared to different matrix element calculations matched to parton shower programs, will provide important feedback for the implementation of Monte Carlo tools, fundamental for the LHC.

8 Acknowledgements

I would like to thank the organizers of the Conference for their kind invitation, and also aknowledge the members of the CDF and DØ Collaborations for their works in achieving the results reported in this contribution.

References

1. The CDF Collaboration, D. Acosta *et al.*, Phys.Rev.D **71**, 032001 (2001).
2. T. LeCompte ant H.T. Diehl, Annu.Rev.Nucl.Part.Sci. **50**, 71 (2000).

3. The CDF Collaboration, T. Affolder *et al.*, Phys.Rev.D**64**, 032001 (2001).
The DØ Collaboration, B. Abbott *et al.*, Phys.Rev.Lett.**82**, 2451 (1999).

4. J. Huston *et al.*, Phys.Rev.Lett. **77**, 444 (1996).

5. J. Pumplin *et al.*, JHEP**0207**, 012 (2002).

6. A.D. Martin *et al.*, Phys.Rev.B **604**, 61 (2004).

7. S. Catani *et al.*, Nucl.Phys.B **406** 187 (1993).
S.D. Ellis and D.E. Soper, Phys.Rev.D **48**, 3160 (1993).

8. G.C. Blazey *et al.*, hep-ex/0005012.

9. S.D. Ellis *et al.*, Phys.Rev.Lett. **64**, 2121 (1990).

10. T. Sjostrand *et al.*, Comput.Phys.Commun.**135**, 238 (2001).

11. The CDF Collaboration, T. Affolder *et al.*, Phys.Rev.D **65**, 092002 (2002).

12. The CDF Collaboration, D. Acosta *et al.*, Phys.Rev.D **71**, 112002 (2005).

13. G. Corcella *et al.*, JHEP **0101**, 010 (2001).

14. W.T. Giele, W.N. Glover and D.A. Kosower, Nucl.Phys.B **403** 633 (1993).

15. A. Bhatti *et al*, hep-ex/0510047.

16. The DØ Collaboration, hep-ex/0511054.

17. T. Binoth *et al*,Eur.Phys.J. **C2**, 311 (2000).
S. Catani *et al*,JHEP**05**,028(2002).

18. L. Bourhis *et al.*, Eur.Phys.J. **C2**, 529 (1998).

19. F. Abe *et al.* (CDF Collab.), Phys. Rev. Lett. **75**, 1451 (1995).

20. M. Cacciari and P. Nason, Phys. Lett. **89**, 122003-1 (2002).

21. The CDF Collaboration, Phys.Rev.D **71**, 032001 (2005).

22. S. Frixione, M. Mangano, Nucl. Phys. **B483**, 321 (1997).

23. M. Mangano *et al.*, CERN-TH/2002-129, hep-ex/0206293.

24. J. Campbell and R.K. Ellis, Phys.Rev.D**65**, 113007 (2002).

25. F. Maltoni and T. Stelzer, JHEP **0302**, 027 (2003).

26. J.M. Campbell, R.K. Ellis, F. Maltoni, S. Willenbrock, Phys.Rev.D**69**, 074021 (2004).